NITROGEN'S ROLE IN THE DEGRADATION OF CRATERS ON PLUTO.

J.E. Hedgepeth (jhedgepe@uwo.ca)[1], C.D. Neish[1], V.J. Bray[2], [1]Institute for Earth and Space Exploration, The University of Western Ontario (1151 Richmond St, London, ON N6A 3K7, Canada), [2]The Lunar and Planetary Laboratory, The University of Arizona (1629 E University Blvd Tucson, AZ 85721)

Introduction: In 2015, the New Horizons spacecraft showed that Pluto's landscape was comprised of regions that continue to be reshaped by volatile ice (e.g. Sputnik Planitia, [1, 2]. The three dominate volatiles there are carbon dioxide, methane and nitrogen [3]. Of these, nitrogen is a key volatile that acts as an insulator, so it may play a significant role in modifying localized features on Pluto's surface. For example, impact craters are known to viscously relax when the water ice bedrock is sufficiently warmed [4]. Furthermore, the seasonality of the N_2 ice will lead to an erosive N_2 cycle of deposition and sublimation in Pluto's impact craters [4, 5]. If this is occurring, the resulting morphological effects on the landscape should be identifiable in the data New Horizons has acquired. Examining impact craters is a valuable way to quantify this effect, since their initial morphology is well constrained, relative to other surface features.

The recent global topographic map produced for Pluto allows us to conduct a study of the degradation of Pluto's craters similar to those on other icy worlds with atmospheres [6, 7]. Robbins et al. [8, 9] have recently estimated the crater population of Pluto and provided depth-diameter trend lines for Pluto craters using Pluto's morphologically pristine craters. However, more work is needed to study the full effect that nitrogen and other volatiles have on the degradation of Pluto's craters. In this work, we expand on the results of Robbins et al. [8, 9] to include Pluto's degraded craters. We quantify the range of degradation observed on Pluto by measuring the relative depth of these craters. Then we integrate the compositional LEISA data to study the relationship between N_2 abundance and crater degradation.

Methods: We used global mosaics from the PDS archive [10] of Pluto from the LORRI (visible), LEISA (infrared) and DEM data set [6] to map Pluto's surface. In our initial work, we map a region of constant pixel scale and phase angle to ensure consistent crater measurements (**Figure 1**). We plan to expand beyond this region in future work. Craters are identified as pristine or degraded based on the criteria outlined in Robbins et al. [8, 9]; we do not make our own assessment of crater degradation when mapping. Lastly, we do not distinguish between complex and simple craters in our initial work.

After mapping, we use the global N_2 absorption mosaic ($2.15\boldsymbol{\mu m}$) to find the average (and error, σ) N_2 content within each crater; these estimates are derived from the interior of the crater rims. Then the crater sizes and positions are exported. Crater depths are found using the 8-profile technique (**Figure 2**) [11]. The 8-profile technique takes 8 topographic profiles through the center of the crater, each equally spaced apart. We find the maximum rim and minimum floor positions on each side of the eight topographic profiles, and the difference between the two points is the crater depth.

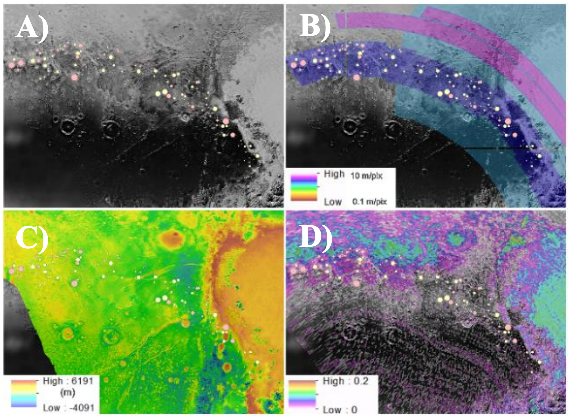

Figure 1. A) Craters mapped as pristine (red) and degraded (yellow) classified in Robbins et al. on a LORRI mosaic [9]. B) Resolution map of the DEM developed by Schenk et al. [6]. C) DEM [6]. D) LEISA N_2 absorption map. The base map is the region mapped in the LORRI mosaic of Pluto (background).

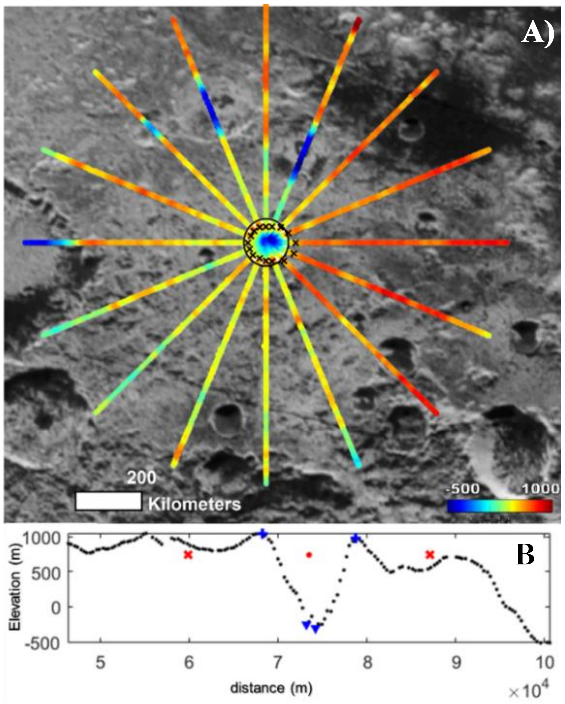

Figure 2. Crater topography is mapped using 8 topographic profiles (A) measuring the rim (blue '+') and floor (blue ∇) (B). The red crosses identify the rim predicted using the LORRI map, and the red dot indicates the center of the crater.

Results and Discussion: Initial results do not show a statistically significant in crater depth compared to N_2 abundance, although shallower craters do qualitatively have higher nitrogen absorption than deeper craters (**Figure 3**). There several things to consider with these results. One, the current dataset only includes craters of $D \geq 10\,km$. Degradation processes may be more prominent in smaller craters. Two, N_2 abundance is at the surface but may not yet have undergone an episode of sublimation. It is the sublimation of N_2 that will trigger erosion and reduce the insolation of the water ice leading to less relaxation [4].

Our initial results do not show that N_2 is more abundant in the degraded craters identified by Robbins et al. [9]. As mentioned above, the shallower craters do show a slightly higher N_2 abundance, but it is largely within the margin of error. The most obvious result is the similarity in depth between the pristine and degraded craters identified by [9] (**Figure 3a**). This suggests that the definition of pristine craters may need to be revised based on their topography data.

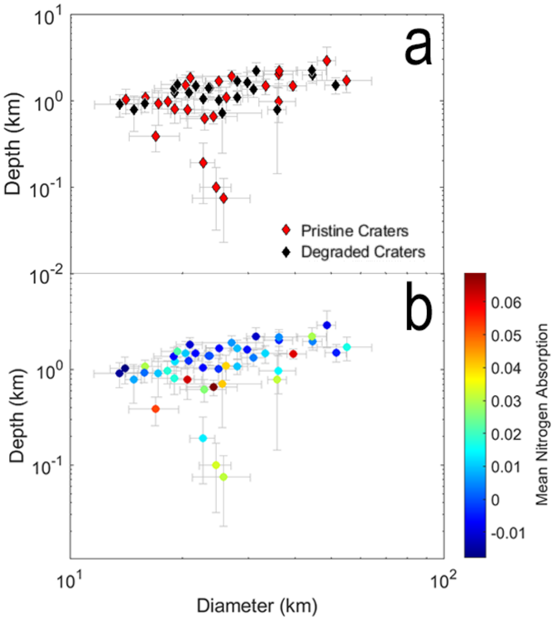

Figure 3. Pluto crater depths compared to crater diameters, a) identified as pristine (red) and degraded (black) based on the results of Robins et al. [9] and b) color-coded by average nitrogen absorption.

It is unclear if the current levels of N_2 are large enough and stable enough to initiate relaxation. We predict that if it is, there should be significantly more degraded larger craters than there are pristine. Modeling work may be needed to test that hypothesis and whether N_2 would be stable enough over geological timescales to accommodate this process. In addition, rim measurements will help to determine whether the shallower craters were degraded by relaxation because rims are often preserved during this process.

Lastly, the measurements of N_2 are surficial, and more buoyant volatiles may float atop larger reservoirs of N_2 ice (i.e. CO_2 or CH_4 in Sputnik Planitia [3]). That is to say, a thin layer CO_2 or CH_4 may cover a deeper reservoir of N_2. LEISA would register CO_2 or CH_4 where it is at the surface even if it overlays a larger N_2 component. We need to study abundances of CO_2 or CH_4 and compare this to the crater morphology to assess whether the N_2 measurements are likely representative of what is really there. Some cases may warrant adding the other volatile abundances to the N_2 abundance measurement to get an accurate estimate of N_2 abundance. This will not ensure the N_2 is stable, but it will offer a constraint for its current distribution. From there, long scale predictions can be made.

Lastly, the current depth distribution will be easier to interpret when converted to relative depths ($R(D) = 1 - \frac{d_{Pluto}(D)}{d_{pristine}(D)}$) to produce a quantitative estimate of crater degradation. Previous works have used similarly sized icy bodies as "pristine" reference points in order to study the degradation of impact craters (e.g. Ganymede as a reference for Titan) [7, 12]. However, Pluto shares no identical twins in size, gravity or composition. In this work, we decided to use Rhea and Oberon as a point of comparison. Rhea and Oberon are slightly smaller (~35%) than Pluto, with lower surface gravities [9], but their crater trend lines provide boundaries for Pluto's craters[13].

Future Work: This work is ongoing, and we plan to complete these steps for all of Pluto's craters with the appropriate DEM and visual data. We also plan to consider the flux of N_2 during its seasonal and diurnal cycles on Pluto. This will constrain how reliable the current snapshot is for the process of crater degradation. Finally, we wish to consider how different N_2 abundances will affect the viscous relaxation of Pluto's craters.

Acknowledgments: J.H. would like to thank the Technologies for Exo-Planetary Science (TEPS) NSERC CREATE program for funding that supported this work.

References: [1] Moore, J. M., et al. (2016) *Science 351*, 1284-1293. [2] McKinnon, W. B., et al. (2016) *Nature 534*, 82–85. [3] Grundy, W. M., et al. (2016). *Science 351*. [4] Stern, S. et al. (2015) *Icarus 250*, 287-293. [5] Bertrand, T., et al. (2018) *Icarus 309*, 277–296. [6] Schenk, P., et al. (2018) *Icarus 314*, 400-433. [7] Hedgepeth, J. E., et al. (2020) *Icarus 344*. [8] Robbins, S., et al. (2017) *Icarus 287*, 187–206. [9] Robbins, S., et al. (2021) *Icarus 356*. [10] Stern, A., (2018) *V1.0. NASA Planetary Data System*. [11] Robbins, S. J., et al. (2018) *Meteoritics & Plan. Sci. 53*, 583-626. [12] . [12] Neish, C.D. et al. (2013). *Icarus 223*, 82-90. [13] Schenk, P., (1989) *Journal of Geo. Res. 94*, 3813-3832.